Chinese Chemical Letters 34 (2023) 108163

Contents lists available at ScienceDirect

Chinese Chemical Letters

journal homepage: www.elsevier.com/locate/cclet

Asymmetric molecular engineering in recent nonfullerene acceptors for efficient organic solar cells

Jinsheng Song[a,*], Zhishan Bo[b,c,*]

[a] Engineering Research Center for Nanomaterials, Henan University, Kaifeng 475004, China
[b] Beijing Key Laboratory of Energy Conversion and Storage Materials, College of Chemistry, Beijing Normal University, Beijing 100875, China
[c] College of Textiles & Clothing, Qingdao University, Qingdao 266071, China

ARTICLE INFO

Article history:
Received 2 December 2022
Revised 30 December 2022
Accepted 26 January 2023
Available online 27 January 2023

Keywords:
Asymmetric strategy
Organic photovoltaics
Nonfullerene acceptor
Side chain engineering
Y-series acceptors

ABSTRACT

Nonfullerene acceptors (NFAs), which usually possess symmetric skeletons, have drawn great attention in recent years due to their pronounced advantages over the fullerene counterparts. Moreover, breaking the symmetry of NFAs could fine tune the molecular dipole, solubility, energy level, intermolecular interaction, molecular packing, crystallinity, *etc*., and give rise to improved photovoltaic performance. Currently, there are three main strategies for the design of asymmetric NFAs. This review highlights the recent advances of high-performance asymmetric NFAs and briefly outlooks the materials exploration for the future.

1. Introduction

Nonfullerene acceptor (NFA) as a new spark in the organic photovoltaic field breaks the long-term domination of the fullerene-based acceptors. In the past three years, great efforts have been devoted to the material design and the power conversion efficiencies (PCEs) of OSCs have been dramatically improved to over 19%, which has significantly surpassed the fullerene counterpart. The state-of-the-art NFAs are generally with a symmetry molecular skeleton to achieve the ordered molecular packing and form the efficient charge transporting channels. The molecules are commonly composed of three main segments: symmetric central conjugated electron-donating cores (D), outstretched side chains and two identical terminal electron-withdrawing end-groups (A). Chemists have conceived a variety of molecular engineering strategies on these three moieties [1,2], which great assisted the fast advance of organic photovoltaic (OPV) field.

While, the strategy of symmetry breaking has been widely adopted in the field such as electro-optics [3], dye-sensitized solar cells [4] and light-emitting diode [5], where asymmetric conjugated skeletons are constructed to generate strong dipoles, produce efficient charge transfer, tune the molecular aggregation, improve the solubility *etc*. Consequently, the absence or violation of symmetry at the three moieties of NFAs that are either expected to have significant impacts on the final molecular systems. Some early works were tried in the D-A small molecule [6] and perylenediimide acceptor [7], but researchers have not noticed the great potential of the asymmetric strategy at that stage due to the moderate photovoltaic performances of these molecular systems. Recently, the asymmetric molecular engineering is also applied on A-D-A-typed NFAs, which brings strong molecular dipole, induces antiparallel packing, forms enhanced π-π stacking, produces efficient charge transport channel, adjusts the processability, achieves preferred morphology, *etc*. The asymmetric molecule strategy has also been verified among the A-DA'D-A-typed Y-series acceptors and PCE of 19% has been achieved [8–12].

Generally, there are three mainstreams for the asymmetric strategy application in NFAs design: (1) asymmetric lateral chains, (2) asymmetric conjugated centers and (3) asymmetric electron deficient terminals. Additionally, some new emerged application in asymmetric polymeric acceptors are also included. In this review, the asymmetric molecules and the corresponding photovoltaic performances have been summarized and analyzed in Table 1; the challenges existing in the future molecular design for these asymmetric acceptors are discussed.

* Corresponding authors.
E-mail addresses: songjs@henu.edu.cn (J. Song), zsbo@bnu.edu.cn (Z. Bo).

https://doi.org/10.1016/j.cclet.2023.108163
1001-8417/

Table 1
Energy levels and photovoltaic details for the asymmetric acceptors.

Acceptor	Active layer	HOMO (eV)	LUMO (eV)	E_g (eV)	Polymer	V_{oc} (V)	J_{sc} (mA/cm^2)	FF	PCE (%)	Ref.
IDT-OB	Binary	−5.77	−3.87	1.66	**PBDB-T**	0.88	15.91	0.70	10.12	[13]
IDTT-OB	Binary	−5.59	−3.88	1.59	**PBDB-T**	0.91	16.41	0.74	11.19	[14]
FOC2C6–2FIC	Binary	−5.51	−3.84	1.43	**PBDB-T**	0.87	19.66	0.72	12.36	[15]
PCBM-C6	Binary	−5.26	−3.84	1.43	**PBDB-T**	0.86	20.41	0.71	12.51	[16]
PCBM-C10	Binary	−5.27	−3.84	1.41	**PBDB-T**	0.87	21.30	0.73	13.55	[16]
C6-IDTT-T	Binary	−5.71	−3.78	1.82	**PTB7-Th**	1.05	14.42	0.56	8.51	[17]
M14	Binary	−5.64	−3.97	1.45	**PM6**	0.89	24.16	0.77	16.46	[18]
ITDI	Binary	−5.89	−4.18	1.53	**PBDB-T**	0.94	13.94	0.60	7.82	[19]
MeIC1	Binary	−5.59	−3.89	1.54	**PBDB-T**	0.93	18.32	0.74	12.58	[20]
IDT6CN-M	Binary	−5.62	−3.90	1.63	**PBDB-T**	0.92	15.97	0.76	11.23	[22]
IDT8CN-M	Binary	−5.54	−3.91	1.58	**PBDB-T**	0.92	17.11	0.79	12.43	[21]
TPTT-IC	Binary	−5.78	−3.95	1.63	**PBT1-C**	0.96	15.50	0.69	10.30	[23]
IDST-4F	Binary	−5.59	−4.01	1.41	**PM6**	0.82	24.90	0.70	14.30	[24]
WA1	Binary	−5.65	−3.97	1.47	**PBDB-T**	0.86	22.65	0.79	15.45	[25]
SePT-IN	Binary	−5.77	−4.00	1.54	**PBT1-C**	0.85	16.37	0.73	10.20	[26]
IPT-2F	Binary	−5.51	−3.96	1.44	**PBDB-T**	0.86	22.40	0.72	14.00	[27]
MQ6	Binary	−5.61	−3.95	1.35	**PM6**	0.88	24.62	0.76	16.39	[33]
IT-3F	Binary	−5.62	−3.51		**PM6**	0.90	20.02	0.73	13.41	[35]
***a*-IT-2OM**	Binary	−5.61	−3.92	1.63	**PBDB-T**	0.93	18.11	0.72	12.07	[34]
IDTT-Cl-2F	Binary	−5.42	−3.92	1.50	**PBDB-T-2Cl**	0.96	19.20	0.71	13.30	[36]
IDTT-Br-2F	Binary	−5.79	−3.99	1.58	**PM6**	0.94	18.40	0.69	12.10	[37]
ZITI-3F	Binary	−5.64	−3.76	1.50	**J71**	0.90	20.67	0.72	13.15	[38]
Y6–1O	Binary	−5.71	−3.84	1.43	**PM6**	0.89	23.20	0.78	16.10	[40]
Y6–1O:PC71BM	Ternary	––			**PM6**	0.90	24.90	0.79	17.60	[40]
EH-HD-4F	Binary	−5.69	−4.04	1.39	**PM6**	0.84	27.50	0.79	18.38	[41]
BTP-PhC6-C11	Binary	−5.74	−4.01	1.33	**PM1**	0.87	26.62	0.79	18.33	[42]
BP5T-4F	Binary	−5.63	−3.88	1.34	**PM6**	0.89	24.60	0.76	16.70	[43]
ABP4T-4F	Binary	−5.65	−3.85	1.37	**PM6**	0.92	22.00	0.75	15.20	[43]
L5	Binary	−5.59	−3.93	1.43	**PBDB-T**	0.86	24.67	0.71	15.20	[44]
L5:Y6	Ternary	––			**PM6**	0.87	27.81	0.71	17.14	[44]
NQF	Binary	−5.62	−3.87	1.43	**PM6**	0.92	25.79	0.74	17.57	[45]
LL3	Binary	−5.48	−3.78	1.70	**PBDB-T**	0.86	26.97	0.72	16.82	[46]
BTP-2F-ThCl	Binary	−5.70	−3.99	1.34	**PM6**	0.87	25.38	0.77	17.06	[47]
BO-5Cl	Binary	−5.62	−3.86	1.76	**PM6**	0.96	22.57	0.70	15.02	[49]
BO-5Cl:BO-4Cl	Ternary	––			**PM6**	0.87	26.93	0.79	18.56	[49]
BTP-S1	Binary	−5.55	−4.01	1.49	**PM6**	0.93	22.39	0.73	15.21	[48]
BTP-S2	Binary	−5.65	−4.01	1.48	**PM6**	0.95	24.07	0.72	16.37	[48]
BTP-2F2Cl	Binary	−5.63	−3.69	1.49	**PM1**	0.86	27.35	0.80	18.40	[9]
BTP-2F2Cl:L8-BO	Ternary	––			**PM1**	0.88	27.15	0.78	19.17	[9]
BTP-S8	Binary	−5.63	−4.09	1.54	**PM6**	0.85	26.96	0.75	17.33	[50]
BTP-S9	Binary	−5.63	−4.09	1.54	**PM6**	0.85	26.72	0.77	17.50	[8]
BTP-S9:BTP-S14	Ternary	––			**PM6**	0.85	27.16	0.78	18.10	[8]
PA1-*o*	Binary	−5.74	−3.83	1.39	**PM6**	0.93	23.99	0.72	16.00	[52]
PY3Se-1V	Binary	−5.51	−3.90	1.25	**PBDB-T**	0.81	24.70	0.66	13.20	[53]

2. Asymmetric molecular strategies: classification and application

2.1. The strategy I: asymmetric lateral chains

To achieve ideal nanoscale phase separation for the active layer of organic solar cells, the polymer donor should precipitate first and form a fibrous network to prevent the small-molecular acceptor from generating large domains. The competitive crystallization processes for the polymer donor and small-molecular acceptor would directly impact the morphology quality. To satisfy the above requirement, the small-molecular acceptor should have a good solubility in the processing solvent, a relatively slow crystallization rate during the drying of the active layer. As known, side chain engineering is a widely used method to adjust the molecular solubility. In 2017, Bo *et al.* firstly designed a kind of asymmetric A-D-A type fused-ring electron acceptor **IDT-OB**, bearing asymmetric side chains at the same sp^3 bridged carbon (one alkyl and one aryl lateral chains) [13]. Such strategy breaks the molecular symmetry without interference with the conjugation characteristics, guarantees good solubility during the processing, enables the acceptor molecules to pack closely in a dislocated way, and provides favorable phase separation when blended with **PBDB-T**. Interestingly, such asymmetric **IDT-OB** based OSCs could achieve high photovoltaic performance thick-film devices (9.17% at thickness of 210 nm). When the IDT core in **IDT-OB** is replaced by a larger conjugated counterpart IDTT, even better performance thick-film devices could be obtained by **IDTT-OB** (10.20% at thickness of 250 nm) [14]. Additionally, this asymmetric side chain strategy is not only effective in the fused ring A-D-A acceptors, it is also applicable in noncovalently fused-ring electron acceptors (NC-FREAs). Bo *et al.* applied this asymmetric strategy to the simple NC-FREAs and a high-power conversion efficiency (PCE) of 12.36% is achieved for **FOC2C6–2FIC** [15]. Recently, Bo and Song rationally designed two novel asymmetric NC-FREAs **PCBM-C6** and **PCBM-C10** *via* unilaterally introducing the phenyl-C_{61}-butyric acid methyl ester (PCBM) as the pendent to fully take advantage of both non-fullerene and fullerene acceptors simultaneously. The bulky, spherical, and electronic isotropic fullerene pendent could effectively suppress severe molecular aggregation, form the preferred blend morphology and further improve the PCE to 13.55% relative to the symmetric control molecule [16].

Besides, side chain tailoring could be another route to fulfill the purpose of asymmetric side chain. Sun *et al.* built one asymmetric wide-bandgap small molecular acceptor **C6-IDTT-T** *via* shearing one hexyl side chain from the end of the donor core and prominent red-shifted absorption is achieved, which should be ascribed to the intense π–π intermolecular interactions in the solid state

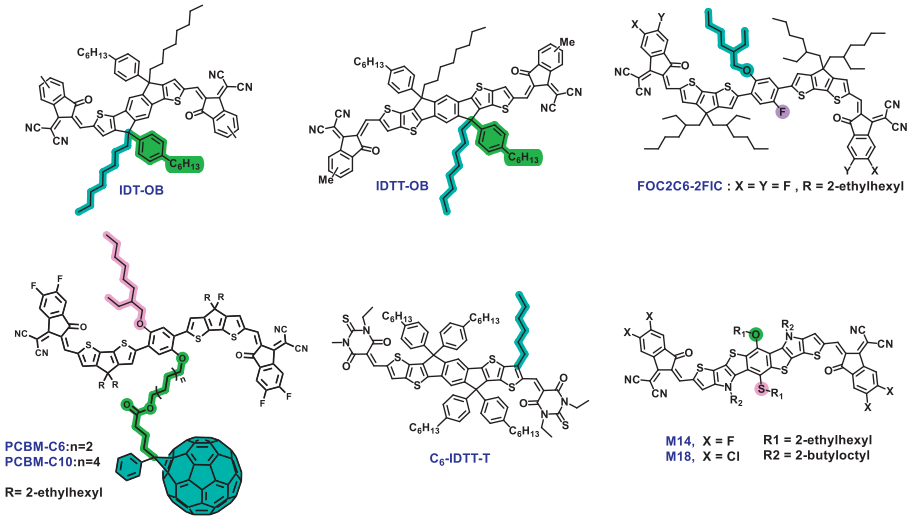

Fig. 1. Representative asymmetric A-D-A-typed NFAs designed *via* strategy I in literature [13–18].

[17]. Very recently, Zheng *et al*. built an asymmetric NFAs **M14** with one alkoxy side-chain and one alkylthio side-chain at the conjugated ladder core, which endows the molecules with increased solubility, enhanced the intermolecular interactions and thereby improved charge transport, and a high PCE 16.46% is achieved by this A-D-A type asymmetric NFAs [18]. In short, though there are not many examples of asymmetric side chains in A-D-A molecules as shown in Fig. 1, the above examples do demonstrate that constructing a ladder-type backbone structure with asymmetric side chains is promising in designing high-performance acceptors with better solubility and more compact molecular packing, which is also especially successful in thickness-insensitive based photovoltaic devices.

2.2. The strategy II: asymmetric conjugated centers

Asymmetric lateral chains mainly improve the processability and tuning molecular packing through changing the surrounding environment of the conjugated skeletons. As the OPV field experienced a long period of development, a variety of symmetric conjugated ladder cores with fused rings have been explored. By tailoring the ladder skeletons from one side, the asymmetric central cores could be acquired and the varied dipole moments between the end group and half of the donor unit will break the dipole counterbalance and induce a new dipole moment for the whole molecule with tunable orientations. IDT and IDTT are the commonly used symmetric ladder core in A-D-A type nonfullerene acceptors and one simple cutting at one sp^3 carbon in the ring (Fig. 2) could introduce asymmetry in the D core, which could be inherited into the final acceptor molecules. For example, Zheng *et al.* developed the indenothiophene core *via* this skeleton shearing strategy and the corresponding **ITDI** molecule presents significantly improved photovoltaic performances in comparison with the symmetric analogue, which also presents good stability for the encapsulated device with 93% initial value after storage for 30 days in air [19].

Ring-fusion could be treated as an alternative molecular design route to achieve the same result as ring-shearing, which alters the core's conjugation length. Yang *et al.* constructed the asymmetric ladder core through the ring-extension by fusing a new thiophene or thieno[3,2-*b*]thiophene unit onto the IDT block [20–22]. As a result, the induced dipoles for **MeIC1**, **IDT6CN-M** and **IDT8CN-M** by asymmetry, strong intermolecular interactions can be generated, leading to a favorable antiparallel packing, high fill factors (FF) of around 80% and the highest PCEs among the OSCs devices. Sun and Yi [23] verified this idea through DFT quantum prediction and found abundant terminal packing probability might exist in the asymmetric molecule aggregates of **TPTT-IC**, two of which (with similar binding energies and more stable configurations) present much stronger intermolecular interactions than that of symmetric one, suggesting that a high electron mobility would be achieved by asymmetric molecules. In some cases, unilaterally inserting one π unit at the symmetric ladder core can also produce asymmetry to the skeleton. Zhang *et al.* utilized the unilateral alkylthio-substituted thiophene unit to construct the asymmetric A-D-π-A acceptor **IDST-4F** [24]. Such structural alteration would induce the dipole change, reinforce the intermolecular interaction, redshift the absorption spectra and achieve a final high PCE of 14.3%. Notably, these devices, displaying improved storage and thermal stability, could retain 82% of the original PCE with no obvious morphological changes after thermal treatment at 150 °C for 1200 min. *Via* moving the phenyl to the lateral terminals, a further enhanced PCE of 15.45% could be achieved by **WA1** [25].

Additionally, the unilateral incorporating heteroatom could also disrupt the skeleton symmetry along with the change of chemical constitution and electronic structure. *Via* the simple replacement of the sulfur atom with the selenium atom, Sun *et al.* reported a new asymmetric analogue to IDT and the corresponding asymmetric acceptor **SePT-IN** presents a bathochromic absorption spectrum, increased intermolecular π-π stacking and a decent PCE of 10.20% in relative to the symmetric counterpart [26]. In some cases, the incorporation of heteroatom is combined with the ring-fusion and side chain engineering. For example, Tang *et al.* [27] reported that the fusion of the thienopyrrole moiety with the IDT unit, which forms a new asymmetric IPT block with an alkyl side chain at the nitrogen atom, whose stronger dipole interactions trigger a closer lamellar packing. It is advantageous to fine-tune the morphology in the active layer for more efficient OSCs by using an S type molecule skeleton as this **IPT-2F** molecule and a more efficient OSCs with a high PCE of 14% is achieved. Afterwards, terminal derivation [28,29] and side chain engineering [30,31] were utilized on this pyrrole modified asymmetric core by several groups. High FF values above 70% are very common for these acceptors and PCEs of ~15% are achieved [28,32]. Zheng *et al.* synthesized the asymmetric **MQ6** bearing a heteroheptacene core with one selenophene heterocycle, which can make best use of the enhanced O···Se noncovalent interaction without interference of the 3D network pack-

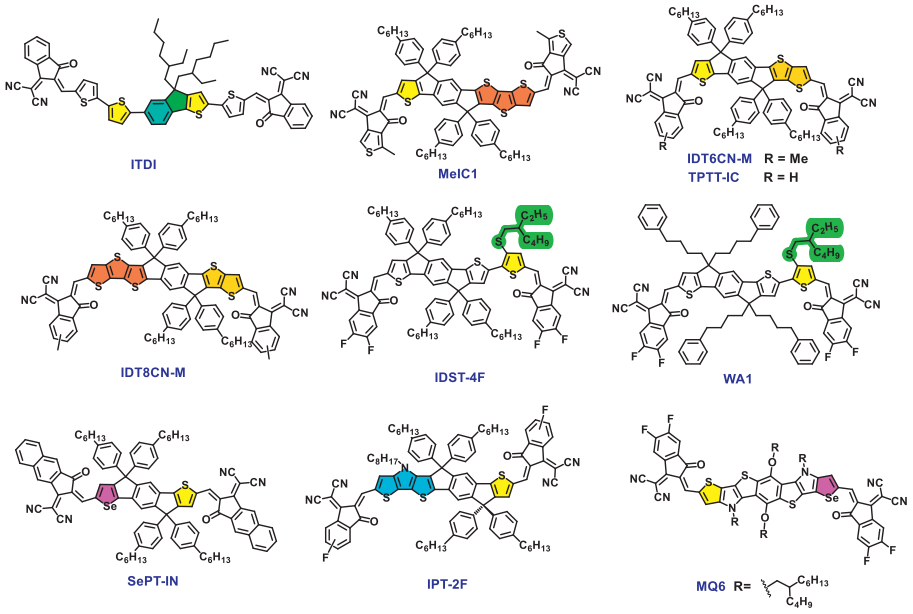

Fig. 2. Representative asymmetric A-D-A-typed NFAs designed *via* strategy II in literature [19–33].

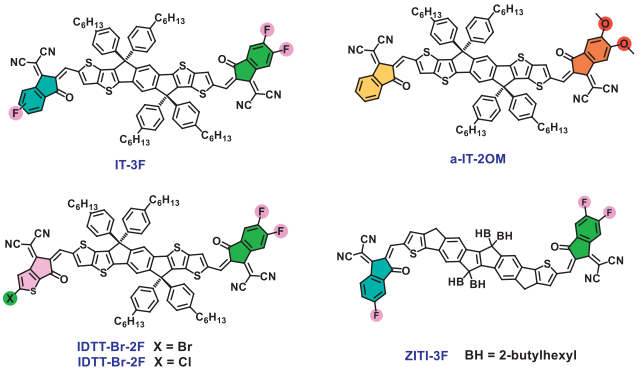

Fig. 3. Representative asymmetric A-D-A-typed NFAs designed *via* strategy III in literature [34–38].

ing in relative to the symmetric counterpart, and a comparable PCE of 16.39% to Y-series acceptors is achieved [33].

2.3. The strategy III: asymmetric electron deficient terminals

Side chain engineering and conjugated skeleton tailoring/fusion would produce conformation asymmetry in the final acceptor molecule and slightly change the electrostatic potential or dipole moment for the whole molecule. In the A-D-A type molecules, the whole and regional dipole moments of the molecules would impact the molecular interactions and aggregation [34] which is directly correlated to the acceptor moieties. Stronger intermolecular dipole interactions have been detected, formed by dipole-driven self-assembly in the NLO molecules previously. Consequently, it would be natural for the researchers to consider utilizing the terminal asymmetric strategy for the A_1-D-A_2 type acceptor molecule design as shown in Fig. 3. Hou *et al.* build the asymmetric molecule **IT-3F** with different F substitution number at each terminal [35] and the corresponding OSCs demonstrated a better photovoltaic performance with a PCE of 13.41% in relative to the symmetric counterparts of **IT-2F** and **IT-4F**. Song *et al.* adopted the consecutive addition method to construct the asymmetric ***a*-IT-2OM**, which combined the general 1,1-dicyanomethylene-3-indanone (IC) with the dimethoxy modified IC. Such molecular design enabled fine tuning of the regional and whole molecular dipole moments, enhancing the intermolecular interactions and achieving encouraging photovoltaic performances by ***a*-IT-2OM** even in thick film devices (>9% at thickness of 450 nm) [34]. Wang *et al.* developed asymmetric acceptors *via* utilizing the synergistic effect of asymmetry and halogenation, which shows the shallowest lowest unoccupied molecular orbital energy level and tight molecular packing from the molecular simulation. When blended with the polymer donors, **IDTT-Cl-2F** [36] and **IDTT-Br-2F** [37] based OSCs yield the PCEs of 12.1% and 13.3%, respectively. Zhu *et al.* reported an asymmetric A–D–A-type nonfullerene **ZITI-3F** based on the dithienocyclopentaindenoindene core [38]. A PCE of 13.15% was achieved by the **J71:ZITI-3F** based devices and further improved PCE of 13.85% was obtained by the "one-pot synthesized composite" due to the synergistic effect and electronic alloy nature of the symmetric and asymmetric moieties. In the meantime, the reversibility of end-group condensation for these asymmetric molecules has been noticed during the synthesis, which may aid the concise preparation of terminal diverse acceptors by one-pot reaction [39]. In short, different D-A terminal combinations would bring varied asymmetry and dipole moments to the whole molecule, ultimately impacting the intermolecular interactions, crystallization properties, blended microscopic morphology and charge transporting process. Though there are only a few A-D-A examples reported utilizing the asymmetric terminal strategy, it is proved to be the most efficient route in Y-series high-efficiency acceptor design (vide infra).

2.4. Application of asymmetric strategies in Y-series acceptors

During the past three years, the fast advance of NFAs has revolutionized the field of OSCs and the photovoltaic performances have been significantly improved to near 19% since the Y-series acceptor have been explored. In the meantime, the three asymmetric strategies for molecular design are also employed during the Y-series acceptor construction as shown in Fig. 4. Yan *et al.* utilized the asymmetric alkyl and alkoxy terminal substitution strategy to balance the solubility and morphology of the final acceptor **Y6–1O**, which finally achieved a PCE of 16.1% and 17.6% in binary and ternary OSCs, respectively [40]. Huang *et al.* introduced asymmetric branched side chains at the nitrogen of the central core of **EH–HD-**

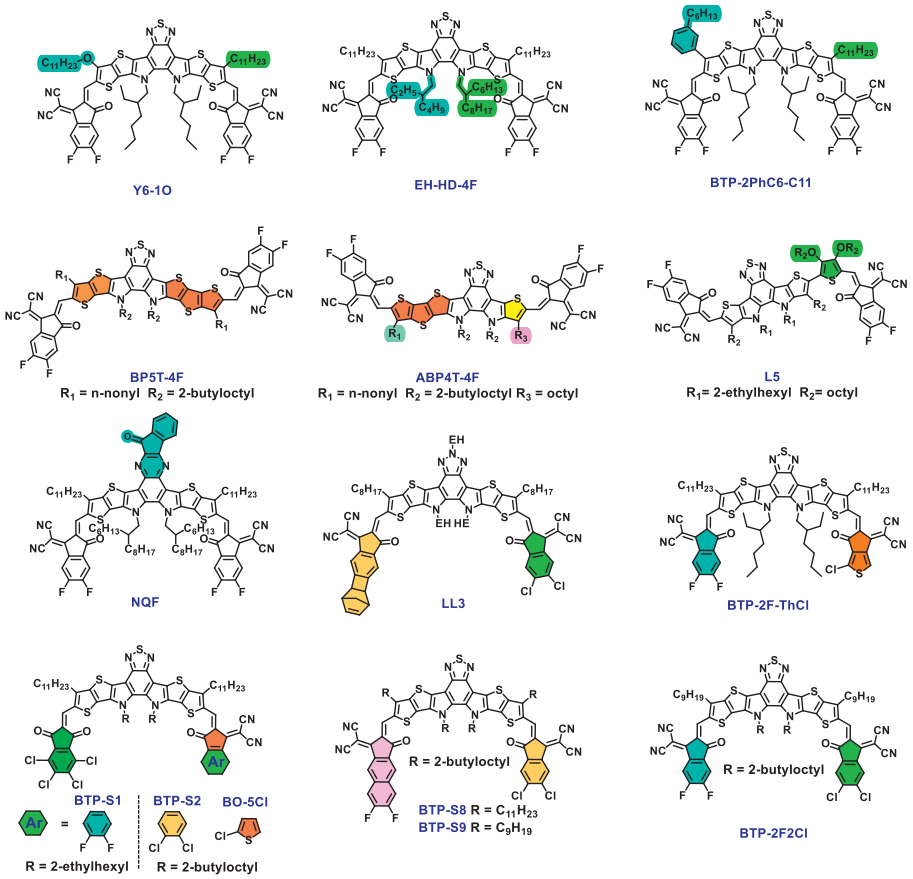

Fig. 4. Representative asymmetric Y-series acceptors in literature [8,9,40-50].

4F, which efficiently affected the absorption spectra, induced more favorable face-on orientation, improved charge transport and reduced recombination losses, and a high PCE of 18.38% with a J_{SC} of 27.48 mA/cm^2 was accomplished by the photovoltaic devices [41]. As mentioned, asymmetric side chain modification on NFAs is an effective and promising method to realize high device efficiencies. Yang *et al.* developed an asymmetric side-chain functionalized Y typed analogues **BTP-PhC6-C11** [42], which enables a 3D network with hydrogen bond assisted crystal packing. The enhanced electronic coupling, larger and more symmetric charge mobility, longer carrier lifetime and enhanced molecular packing guarantees the best photovoltaic performance for the blend based on **BTP-PhC6-C11** with a PCE of 18.33%.

Aiming at the ladder core, Jen *et al.* built asymmetric Y-type acceptors through shearing or fusing one more thiophene unit at the terminal of π-conjugated skeleton and two distinct molecular conformations (Z-shape and W shape) for NFAs (**BP5T-4F** and **ABP4T-4F**) [43] are obtained, which could achieve appropriate micromorphology, suppress the nonradiative recombination loss and give high PCEs of 16.7% and 15.2%, respectively. Bo *et al.* unilateral introduced a thiophene alkoxy units resulting in an asymmetric skeleton of **L5**, which endows the acceptor with a slightly twisted molecular conformation in solution but a planar one in the solid state. Such dynamic transformation properties facilitate the good processability in solution while maintaining a dense molecular packing in a thin film. Hence, the binary as-cast devices based on L5 generate a high PCE of 15.2% and ternary devices of **PM6**:**L5**:**Y6** achieved a higher PCE of 17.14% [44]. Recently, researchers also noticed that high nonradiative recombination energy loss (ΔE_{nr}) is one of the significant factors that limit efficiencies of organic solar cells (OSCs), Chen *et al.* developed an acceptor **NQF** with an asymmetric and extended conjugation at the central electron deficient core [45]. The asymmetry in **NQF** increases the dipole moment of the acceptor and strengthen the rigidity of the molecule, resulting in a high-power conversion efficiency (PCE) of 17.57% with a rather low ΔE_{nr} of 0.177 eV.

As mentioned above, the asymmetric electron terminals would create permanent dipoles in the A-D-A type NFAs and tune the molecular stacking. Very recently, Bo *et al.* developed a three-dimensional shape-persistent CBIC terminal group to pair with the chlorinated IC terminal groups and an asymmetric acceptor **LL3** could be constructed. The novel **LL3** design could effectively improve the solubility and regulated the molecular packing mode as well, which finally reaches a PCE of 16.83% [46]. Through utilizing the thiophene fused terminal (CPTCN–Cl) at one end in **BTP-2F-ThCl**, a minimal energy offset and sufficient charge separation could be achieved, which realizing a PCE approaching 17% with a balance between V_{OC} and J_{SC} [47]. Chen *et al.* demonstrated highly efficient OSCs with improved luminescence *via* the introduction of electron-poor terminals in the asymmetric acceptor molecules **BTP-S1**, **BTP-S2** [48] and **BO-5Cl**, which generates dual nature of the interfacial electronic states and brings combined low non-radiative voltage losses and high charge generation efficiency when the resulted acceptor was used as the third component [49,50]. Encouragingly, some other terminal functionalized asymmetric guest acceptors as **BTP-2F2Cl** [9] and **BTP-S9** [8] could achieve high PCEs around 19% due to the improved the exciton behaviors and reduced energetic disorder, respectively. Additionally, not only the experimental results demonstrate the photovoltaic performance improvement for the asymmetric Y-series acceptors, quantum chemistry prediction also confirms that these asymmetric acceptors possess enhanced light absorption ability, improved

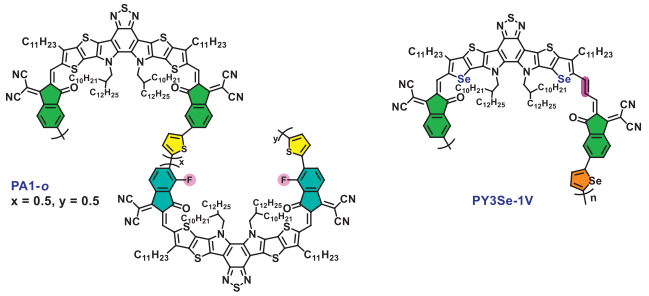

Fig. 5. Examples of asymmetric strategy in PSMAs in literature [52,53].

interfacial properties with more CT states and strong interactions with the donor [51], contributing to such excellent photovoltaic performances.

2.5. Application of asymmetric strategies in polymer acceptors

In the field of electron acceptors, polymer counterpart as another potential branch attracted more attention in organic photovoltaics. Recently, Li *et al.* conceived a new strategy for NFAs design *via* polymerizing the small molecular acceptors (PSMAs) and the widely used monomers are from Y-series acceptors, which achieves good film quality, stable morphology, high absorption coefficients and high photovoltaic performance. During the PSMAs design, they also borrowed the asymmetric concept from small molecular NFAs (Fig. 5). For example, Li *et al.* developed an asymmetry concept for **PA1-*o*** [52] design *via* random polymerization of two different symmetric SMA building blocks with a thiophene linking unit. The **PM6**:**PA1-*o***-based all-PSC achieved the highest PCE of 16.0%, suggesting that asymmetric copolymerization is an effective strategy for synthesizing high-performance PSMAs. Jen *et al.* adopted a vinylene-inserted asymmetric monomer for the preparation of PSMA, **PY3Se-**1V [53], whose absorption onset reached 1000 nm. Due to the enhanced electron-donating ability and quinoidal character of such a DA'D-V-type core, the corresponding asymmetric **PY3Se-**1V with an ultra-low bandgap of 1.25 eV still maintains a moderate LUMO energy level of −3.90 eV and the corresponding all-PSCs based on **PBDB-T**:**PY3Se-**1V achieved a high PCE of 13.2%. Both examples demonstrate the asymmetric strategy could be transplanted to the polymeric PSMAs design for high performance of all polymer solar cells.

3. Conclusion and perspective

In conclusion, the current asymmetric molecular engineering could endow the nonfullerene acceptors with further improved performances by virtue of enhanced dipole, tunable intermolecular interaction, adjustable packing mode, balanced processability, improved luminescence, reduced energetic disorder and *etc.,* and guarantee the final device with thickness insensitivity. Although progressive advancements with remarkable PCEs around 19% have been accomplished by the asymmetric nonfullerene acceptors, the fast advances of this branch are highly dependent on the symmetric counterpart. The key points towards the future exploration may include the following aspects:

(1) Accurate combination rules of these asymmetric strategies are demand to fulfill the fine tune of the processability and crystallinity, charge transportation, staking properties for excellent photovoltaic performances.
(2) The current studies related to the asymmetric acceptors are still lack of crystals and only a few studies include the molecular stacking information; the molecular design combined with the quantum chemistry prediction may provide some deep insights for this strategy.
(3) Systematic guide for the asymmetric molecular design should be devoted more efforts to further understand the impacts of conjugated skeleton, terminal, and side chain type on the detailed photovoltaic parameters.
(4) Take advantage of the intermolecular tunability by this asymmetric strategy and extend it to some newly reported potential systems (*e.g.*, noncovalent fused ring acceptors and fully nonfused acceptors) for intensive study.
(5) Accompany with the development of the asymmetric acceptors, the exploration of donor components either polymers or oligomers should also catch up so as to generate matched and efficient charge transport channels.

Declaration of competing interest

The authors declare that they have no known competing financial interests or personal relationships that could have appeared to influence the work reported in this paper.

Acknowledgments

This work was supported by the National Natural Science Foundation of China (Nos. 22075069, 51933001), Natural Science Foundation of Henan Province (No. 212300410002) and Program sponsored by Henan Province (Nos. 23ZX002, ZYQR201912163).

References

[1] J. Gao, X. Zhu, H. Bao, et al., Chin. Chem. Lett. 34 (2023) 107968.
[2] W. Xu, Y. Chang, X. Zhu, et al., Chin. Chem. Lett. 33 (2022) 123–132.
[3] L.R. Dalton, P.A. Sullivan, D.H. Bale, Chem Rev 110 (2010) 25–55.
[4] A. Mishra, M.K. Fischer, P. Bauerle, Angew. Chem. Int. Ed. 48 (2009) 2474–2499.
[5] H. Wang, L. Xie, Q. Peng, et al., Adv. Mater. 26 (2014) 5198–5204.
[6] P.E. Schwenn, K. Gui, A.M. Nardes, et al., Adv. Energy Mater. 1 (2011) 73–81.
[7] Y. Yin, J. Song, F. Guo, et al., ACS Appl. Energy Mater. 1 (2018) 6577–6585.
[8] L. Zhan, S. Li, Y. Li, et al., Joule 6 (2022) 662–675.
[9] R. Sun, Y. Wu, X. Yang, et al., Adv. Mater. (2022) e2110147.
[10] L. Zhu, M. Zhang, J. Xu, et al., Nat. Mater. 21 (2022) 656–663.
[11] C. He, Y. Pan, Y. Ouyang, et al., Energy Environ. Sci. 15 (2022) 2537–2544.
[12] Y. Cui, Y. Xu, H. Yao, et al., Adv. Mater. 33 (2021) 2102420.
[13] S. Feng, C. Zhang, Y. Liu, et al., Adv. Mater. 29 (2017) 1703527.
[14] S. Feng, C. Zhang, Z. Bi, et al., ACS Appl. Mater. Interfaces 11 (2019) 3098–3106.
[15] S. Feng, M. Li, N. Tang, et al., ACS Appl. Mater. Interfaces 12 (2020) 4638–4648.
[16] Y. Zhou, M. Li, S. Shen, et al., ACS Appl. Mater. Interfaces 13 (2021) 1603–1611.
[17] T. Xia, C. Li, H.S. Ryu, et al., Sol. RRL 4 (2020) 2000061.
[18] Q. Tu, W. Zheng, Y. Ma, et al., CCS Chem. 5 (2023) 455–468.
[19] Z. Kang, S.C. Chen, Y. Ma, J. Wang, Q. Zheng, ACS Appl. Mater. Interfaces 9 (2017) 24771–24777.
[20] W. Gao, Q. An, C. Zhong, et al., Chem. Sci. 9 (2018) 8142–8149.
[21] W. Gao, T. Liu, C. Zhong, et al., ACS Energy Lett. 3 (2018) 1760–1768.
[22] W. Gao, M. Zhang, T. Liu, et al., Adv. Mater. 30 (2018) e1800052.
[23] C. Li, Y. Xie, B. Fan, et al., J. Mater. Chem. C 6 (2018) 4873–4877.
[24] Q. Guo, J. Lin, H. Liu, et al., Nano Energy 74 (2020) 104861.
[25] P. Wang, Y. Li, C. Han, et al., J. Mater. Chem. A 10 (2022) 17808–17816.
[26] C. Li, J. Song, Y. Cai, et al., J. Energy Chem. 40 (2020) 144–150.
[27] L. Yang, X. Song, J. Yu, et al., J. Mater. Chem. A 7 (2019) 22279–22286.
[28] G. Li, D. Li, R. Ma, et al., J. Mater. Chem. A 8 (2020) 5927–5935.
[29] W. Gao, T. Liu, R. Sun, et al., Adv. Sci. 7 (2020) 1902657.
[30] J. Cao, S. Qu, L. Yang, et al., Sci. Bull. 65 (2020) 1876–1879.
[31] J. Cao, H. Wang, S. Qu, et al., Adv. Funct. Mater. 30 (2020) 2006141.
[32] Q. Guo, R. Ma, J. Hu, et al., Adv. Funct. Mater. 30 (2020) 2000383.
[33] C. Tang, X. Ma, J.Y. Wang, et al., Angew. Chem. Int. Ed. 60 (2021) 19314–19323.
[34] M. Li, Y. Zhou, J. Zhang, J. Song, Z. Bo, J. Mater. Chem. A 7 (2019) 8889–8896.
[35] B. Gao, H. Yao, J. Hou, et al., J. Mater. Chem. A 6 (2018) 23644–23649.
[36] J. Cai, X. Zhang, C. Guo, et al., Adv. Funct. Mater. 31 (2021) 2102189.
[37] J. Cai, C. Guo, L. Wang, et al., Org. Electron. 100 (2022) 106357.
[38] J. Zhang, W. Liu, S. Chen, et al., J. Mater. Chem. A 6 (2018) 22519–22525.
[39] T.J. Aldrich, M. Matta, W. Zhu, et al., J. Am. Chem. Soc. 141 (2019) 3274–3287.
[40] Y. Chen, F. Bai, Z. Peng, et al., Adv. Energy Mater. 11 (2020) 2003141.
[41] S. Chen, L. Feng, T. Jia, et al., Sci. China Chem. 64 (2021) 1192–1199.
[42] Z.H. Luo, Y. Gao, H.J. Lai, et al., Energy Environ. Sci. 15 (2022) 4601–4611.
[43] W. Gao, H. Fu, Y. Li, et al., Adv. Energy Mater. 11 (2020) 2003177.
[44] D. Li, H. Lu, Y.N. Chen, et al., Chem. Mater. 34 (2022) 8840–8848.
[45] J. Wang, H. Chen, X. Xu, et al., J. Mater. Chem. A 10 (2022) 16714–16721.

[46] H. Lu, H. Jin, H. Huang, et al., Adv. Funct. Mater. 31 (2021) 2103445.
[47] Z. Luo, R. Ma, T. Liu, et al., Joule 4 (2020) 1236–1247.
[48] S. Li, L. Zhan, Y. Jin, et al., Adv. Mater. 32 (2020) e2001160.
[49] C. He, Z. Chen, T. Wang, et al., Nat. Commun. 13 (2022) 2598.
[50] S. Li, L. Zhan, N. Yao, et al., Nat. Commun. 12 (2021) 4627.
[51] J. Yang, Q.S. Li, Z.S. Li, Phys. Chem. Chem. Phys. 23 (2021) 12321–12328.
[52] J. Du, K. Hu, C. Zhu, et al., Macromolecules 55 (2022) 7481–7487.
[53] Q. Fan, H. Fu, M. Liu, et al., ACS Appl. Mater. Interfaces 14 (2022) 26970–26977.